

Factors Affecting Temporal Variations In Vapor Intrusion-Induced Indoor Air Contaminant Concentrations

Jonathan G. V. Ström^a, Yuanming Guo^b, Yijun Yao^b, Eric M. Suuberg^a

^a*Brown University, School of Engineering, Providence, RI, USA*

^b*Arizona State University, School of Sustainable Engineering and the Building
Environment, Tempe, AZ, USA*

Abstract

Temporal variability in indoor air contaminant concentrations at vapor intrusion (VI) sites has been a concern for some time. We consider the source of the reported variability at VI sites located near Hill Air Force Base (AFB) in Utah, an EPA experimental house in Indiana, and Naval Air Station North Island in California. We focus in particular on how the indoor/outdoor pressure differences and air exchange rates affected indoor air contaminant concentrations at these sites. We investigate how these dynamics differ for a site that is characterized by a preferential pathway (like Hill AFB) and VI sites that are not influenced by such pathways, using three-dimensional fluid dynamics models and statistical analysis of the aforementioned sites. A preferential pathway can dramatically increase a VI site's sensitivity to build pressurization, provided there exist a medium allowing effective communication between a contaminant-delivering preferential pathway and the indoor air space, e.g. a permeable subslab space that may be provided by a gravel layer. Preferential pathways may also erroneously indicate the presence of indoor contaminant sources. At sites characterized by significant advective transport from the subslab to the indoor air space, much of the short-term variability in indoor air contaminant concentration can be explained by an impact of fluctuations in indoor/outdoor pressure differences. Meanwhile, air exchange rate variation drives most of the short-term variability at sites characterized by minor variations in advective transport.

Keywords: Vapor intrusion, Preferential pathways, Temporal variability,
Attenuation factor, Air exchange rate, Indoor/outdoor pressure difference

1. Introduction

Long term vapor intrusion (VI) studies in both residential and larger commercial structures have raised concerns regarding significant observed transient behavior in indoor air contaminant concentrations[1, 2, 3, 4, 5, 6, 7]. Such variations make it difficult for those charged with protecting human health to formulate a response - should evaluation of the risk of exposure be based upon observed peak concentrations, or long-term averages, or something else? There is even uncertainty within the VI community regarding how to best develop sampling strategies to address this problem[1, 3, 8]. What represents a reasonable sampling strategy for a particular site a single 8-hour sample? Repeated 8-hour samples? Month-long samples? Continuous monitoring?

VI involves the migration of volatilizing contaminants from soil, groundwater or other subsurface sources into overlying structures. The basic nature of VI has been understood for some time and it has been the subject of much study, but some aspects remain poorly understood, such as the causes of the sometimes observed large temporal transients in indoor air concentrations. Results from a house operated by Arizona State University (ASU) near Hill AFB in Utah, an EPA experimental house in Indianapolis, IN and a large warehouse at the Naval Air Station (NAS) North Island, CA have all shown significant transient variations in indoor air contaminant concentrations. All were outfitted with sampling and monitoring equipment that allowed tracking temporal variation in indoor air contaminant concentrations on time scales of hours. All have shown that these concentrations vary significantly with time - orders of magnitude on the timescale of a day or days[9, 10, 5].

In one instance the source of the variation was clearly established during the study of the site. At the ASU house a drain pipe (or “land drain”) connected to a sewer system was discovered beneath the house. Careful isolation of this source led to a clear conclusion that this “preferential pathway” for contaminant vapor migration significantly contributed to observed indoor air contaminant levels and their fluctuations[10, 11]. While in this case the issue of a contribution from a preferential pathway was clearly resolved, what it left open was a question of whether existence of such a preferential pathway would always be expected to lead to large fluctuations in indoor air contaminant concentrations.

Similarly, a sewer pipe has recently been suggested to be a source of the contaminants found in the EPA Indianapolis house. That site was also characterized by large indoor air contaminant concentration fluctuations[12, 7]. Sewer lines have been previously implicated as VI sources at several sites[13, 12, 14, 15]. A Danish study has estimated that roughly 20% of all VI sites in central Denmark involve significant sewer VI pathways[16]. Thus while consideration of sewer or other preferential pathways is now part of normal good practice in VI site investigation[1], it is still not known whether the existence of such pathways automatically means that large temporal fluctuations are necessarily to be expected.

In some of the above cited cases[13, 15], a sewer provided a pathway for direct entry of contaminant into the living space. While potentially important in many instances, this scenario is not further considered here where the focus is on pathways that deliver contaminant via the soil beneath a structure. It is, however, now known that even absent a preferential pathway, there may be significant transient variation in indoor air contaminant concentrations at VI sites[2, 17, 4]. One example is the site at NAS North Island at which no preferential pathways have been identified. Instead, a building at this site is characterized by significant temporal variations in indoor-outdoor pressure differential[5]. It is believed that this is the origin of the observed indoor air contaminant concentration fluctuations at that site.

This paper investigates the sources of the temporal variation in indoor air contaminant concentrations in both the presence and absence of preferential pathways. In this work, the latter scenarios are referred to as “normal” VI scenarios, in which there is typically a groundwater source of the contaminant. Specifically, we pose the question of just how much variation in indoor air contaminant concentration may be expected at such normal VI sites vs. those characterized by preferential pathways within the soil beneath the site. The conditions required for preferential pathways to become significant contributors to temporal variations in indoor air contaminant concentrations are also explored, and the consequences for sampling strategies are discussed.

2. Methods

2.1. Statistical Analysis Of Field Data

To frame the question of just how much variability in indoor air contaminant concentrations is actually observed, field datasets have been analyzed. For this purpose, datasets from the ASU house in Utah, the EPA

Indianapolis site and North Island NAS were chosen for analysis. Readers are referred to the original published works for details regarding data acquisition[9, 10, 3, 5, 7].

The ASU house data were obtained over a period of several years. During part of this time, controlled pressure method (CPM) tests were being conducted, in which the house was underpressurized to an extent greater than that characterizing “normal” house operation: increasing VI potential[18, 6, 9]. The period of CPM testing is thus excluded from the analysis. Likewise, the existence of a preferential pathway at the ASU house needs to be considered in examining that dataset; during some of the testing at that site, this pathway was cut off, resulting in “normal” VI conditions in which the main source of contaminant was diffusion of contaminant vapor from an underlying groundwater source.

The NAS North Island dataset has not (as far as is known) been influenced by a preferential pathway, but the structure there was subject to “large” internal pressure fluctuations. By “large” is meant still only of order 10-20 Pa, but these were greater than those generally recorded at the ASU house during normal operations. The underlying soil at NAS North Island is sandy[5] and more permeable than that at the ASU site, which will be shown to lead to greater pressure sensitivity in the former case.

The Indianapolis site investigation also spanned a number of years and periodically included the testing of a sub-slab depressurization system (SSD) for VI mitigation. Only the period before the installation of this system was considered in the present analysis. It is likely a sewer line beneath the structure acted as a preferential pathway[12]. Unlike at the ASU house, this preferential pathway was never removed or blocked, making it impossible to isolate the role of the preferential pathway at this site. It is still of interest to consider the data from this site because of the completeness and extensiveness of the data collection. Figure 1 illustrates a typical reported series of indoor air trichloroethylene (TCE) concentration measurements from this site. There is almost a two order of magnitude variation in the concentration data.

Some of the analysis of the above three field data sets relies on a probability density estimation technique called “kernel density estimation” (KDE). KDE is a technique used for estimating the probability distribution of a random variable(s) by using multiple kernels, or weighting functions to characterize the data sets. In this case, Gaussian kernels are used to create the KDEs. This means that it is presumed that the variables of interest (i.e.,

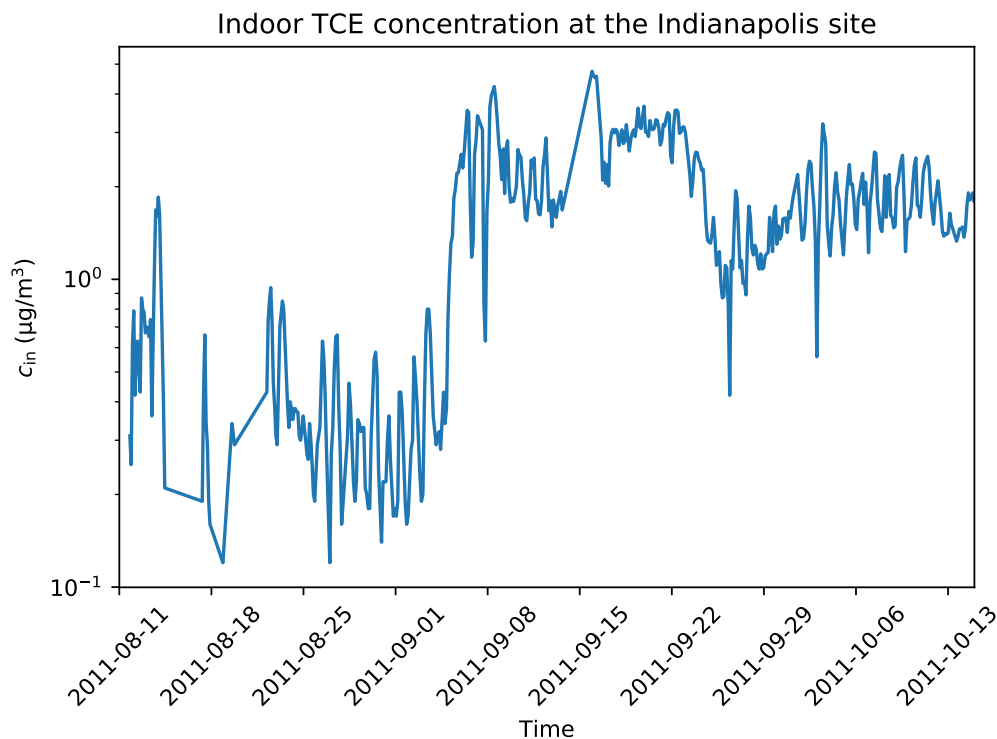


Figure 1: Typical data on indoor air TCE contaminant concentrations at the Indianapolis site[7].

120 indoor air contaminant concentrations and indoor-outdoor pressure differ-
 121 entials, as sampled) are normally distributed around mean values and that
 122 there are statistical fluctuations associated with each sampling event. In this
 123 instance, the scipy statistical package was used to construct the KDEs, as-
 124 suming a bandwidth parameter determined by Scott’s rule. The SciPy Python
 125 library was used to conduct all statistical analysis and data processing[19].

126 2.2. Modeling Work

127 A previously described three-dimensional computational fluid dynamics
 128 model of a generic VI impacted house has been used to elucidate certain
 129 aspects of transient VI processes. In the present work, there has been an
 130 addition of a preferential pathway to the “standard” model that has been
 131 described before in publications by this group[20, 21, 22]. As in the earlier

132 studies, only the vadose zone soil domain is directly modeled. Figure 2 shows
 133 a cutaway view of the relevant modeling domain.

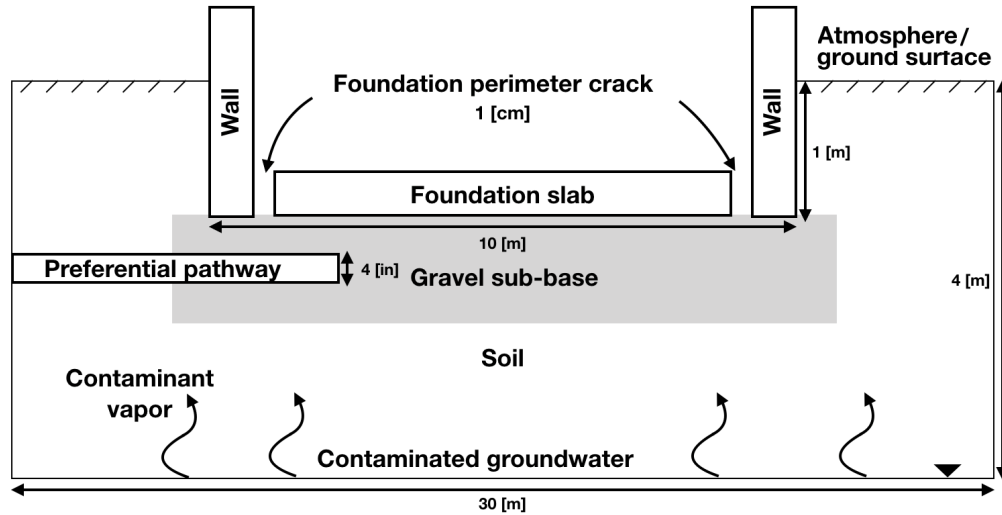


Figure 2: Foundation and vadose zone soil represented in the modeling. Note that here a gravel sub-base material is shown, but in certain simulations, that material is absent and the surrounding soil directly contacts the foundation slab. Different assumptions are made regarding the preferential pathway, here shown as a pipe entering the gravel sub-base. In some cases, the preferential pathway has been "turned off".

134 The modeled VI impacted structure is assumed to have a 10x10 m founda-
 135 tion footprint, with the bottom of the foundation slab lying 1 m below
 136 ground surface (bgs), simulating a house with a basement. The indoor air
 137 space is modeled as a continuously stirred tank (CST)[1] and all of the con-
 138 taminant entering the house is assumed to enter with soil gas through a 1
 139 cm wide crack located between the foundation walls and the foundation slab
 140 around the perimeter of the house. All of the contaminant leaving the in-
 141 door air space is assumed to do so via air exchange with the ambient. The
 142 indoor control volume is here assumed to consist of only of the basement,
 143 having a total volume of 300 m³. Clearly different assumptions could be
 144 made regarding the structural features and the size of the crack entry route,
 145 but for present purposes, this is unimportant as the intent is only to show
 146 for "typical" values what the influence of some critical parameters is.

147 The modeled surrounding soil domain extends 5 meters from the perime-
 148 ter of the house and is assumed to consist of sandy loam, except as noted

149 otherwise. Directly beneath the foundation slab, there is assumed to be a 30
 150 cm (one foot) thick gravel layer, except in certain cases here this sub-base
 151 material is assumed to be the same as the surrounding soil (termed a "uni-
 152 form" soil scenario). The groundwater beneath the structure is assumed to
 153 be homogeneously contaminated with TCE selected as a prototypical con-
 154 taminant. The groundwater itself is not modeled, as the bottom of the
 155 model domain is defined by the top of the water table. Where relevant, the
 156 preferential pathway is modeled as a 10 cm (4") pipe that opens into the
 157 gravel sub-base beneath the structure. The air in the pipe is also assumed
 158 to be contaminated with TCE at a vapor concentration equal to the vapor
 159 in equilibrium with the groundwater contaminant concentration below the
 160 structure, modified by a scaling factor χ (allowing the contaminant concen-
 161 tration in the pipe to be parameterized). This model illustrates the concept
 162 of a "preferential pathway", as the pipe carries contaminant vapor to the
 163 immediate vicinity of the foundation, by a path that circumvents the usual
 164 soil diffusion pathway.

165 The ground surface and the pipe are both sources of air to the soil domain.
 166 Both are assumed to exist at reference atmospheric pressure. Soil gas trans-
 167 port is governed by Richard's equation, a modified version of Darcy's Law,
 168 taking the variability of soil moisture in the vadose zone into account[23].
 169 The van Genuchten equations are used to predict the soil moisture content
 170 and thus the effective permeability of the soil[24]. The effective diffusivity
 171 of contaminant in soil is calculated using the Millington-Quirk model[25].
 172 The transport of contaminant vapor in the soil is assumed to be governed by
 173 the advection-diffusion equation, in which either advection or diffusion may
 174 dominate depending upon position and particular circumstances. The key
 175 working equations and the boundary conditions are summarized in Table 1.

| Governing Equations | | | | | |
|---|---|------------------------------------|--|-----------------------------------|-------|
| Unsteady-CST | $V \frac{dc_{in}}{dt} = \int_{A_{ck}} j_{ck} dA - c_{in} A_e V_{slab}$ | | | | |
| Richard's | $\nabla \cdot \rho \left(-\frac{\kappa_s}{\mu} k_r \nabla p \right) = 0$ | | | | |
| Transport | $\frac{\partial}{\partial t} \left(\theta_w c_w + \theta_g c \right) = \nabla (D_{eff} \cdot \nabla c) - \vec{u} \cdot \nabla c$ | | | | |
| Millington-Quirk | $D_{eff} = D_{air} \frac{\theta_g^{10/3}}{\theta_t^2} + \frac{D_{water}}{K_H} \frac{\theta_w^{10/3}}{\theta_t^2}$ $Se = \frac{\theta_w - \theta_r}{\theta_t - \theta_r} = [1 + \alpha z ^n]^{-m}$ | | | | |
| van Genuchten | $\theta_g = \theta_t - \theta_w$ | | | | |
| | $k_r = (1 - Se)^l [1(Se^m)^m]^2$ $m = 1 - 1/n$ | | | | |
| Boundary Conditions | | | | | |
| Boundary | Richard's Eqn. | | Transport Eqn. | | |
| Foundation crack | $p = p_{in/out} \text{ (Pa)}$ | | $j_{ck} = \frac{uc}{1 - \exp(uL_{slab}/D_{air})}$ | | |
| Groundwater | <i>No flow</i> | | $c = c_{gw} K_H \text{ (}\mu\text{g/m}^3\text{)}$ | | |
| Ground surface | $p = 0 \text{ (Pa)}$ | | $c = 0 \text{ (}\mu\text{g/m}^3\text{)}$ | | |
| Preferential pathway | $p = 0 \text{ (Pa)}$ | | $c = c_{gw} K_H \chi \text{ (}\mu\text{g/m}^3\text{)}$ | | |
| Soil Properties[26, 27, 28] | | | | | |
| Soil | $\kappa_s \text{ (m}^2\text{)}$ | θ_s | θ_r | $\alpha \text{ (1/m)}$ | n |
| Gravel | $1.3 \cdot 10^{-9}$ | 0.42 | 0.005 | 100 | 3.1 |
| Sandy Loam | $5.9 \cdot 10^{-13}$ | 0.39 | 0.039 | 2.7 | 1.4 |
| Trichloroethylene (diluted in air) Properties[27, 28] | | | | | |
| | $D_{air} \text{ (m}^2\text{/h)}$ | $D_{water} \text{ (m}^2\text{/h)}$ | $\rho \text{ (kg/m}^3\text{)}$ | $\mu \text{ (Pa} \cdot \text{s)}$ | K_H |
| | $2.47 \cdot 10^{-2}$ | $3.67 \cdot 10^{-6}$ | 1.614 | $1.86 \cdot 10^{-5}$ | 0.403 |
| Building Properties | | | | | |
| | $V_{base} \text{ (m}^3\text{)}$ | $L_{slab} \text{ (cm)}$ | $A_e \text{ (1/hr)}$ | | |
| | 300 | 15 | 0.5 | | |

Table 1: Governing equations, boundary conditions & model input parameters. See Table 4 for nomenclature.

176 3. Results & Discussion

177 3.1. Variation In Indoor Air Contaminant Concentration Over Time

178 High frequency measurement of indoor air contaminant concentrations,
179 c_{in} , such as those in Figure 1, took place at both the ASU House and the

Indianapolis House over significant periods (Indianapolis: ca 1.7 years, ASU house: ca 3.5 years)[7, 3]. Furthermore, at the Indianapolis site c_{in} for three different contaminants, chloroform, TCE, and tetrachloroethylene (PCE) were all collected, allowing examination of the variability of each VI contaminant. The NAS North Island NAS dataset was obtained over a much shorter duration (9 days), and is therefore not examined in this portion of the analysis. It should also be noted that the ASU house used 4-hour sorbent tubes, while Indianapolis took instantaneous "grab" samples.

Figure 1 showed a large degree of temporal variation in one of the components, and the data for the other components were quite similar. What is apparent upon closer examination of such data is that the actual day-to-day variations are typically not nearly as large as those observed when tracking the data for a longer time. To demonstrate this point, the quotient of the maximum and minimum c_{in} values (denoted as c_{max}/c_{min}) are shown as a function of time in Figure 3. The values shown in Figure 3 are the means of the quotients calculated for samples separated by the indicated times and the error bars indicate the 95th percentile of all the data points. Hypothetical resampling periods of one, two, three days, and the same number of weeks, and months were chosen.

For example, if the data are examined in terms of the mean maximum variation observable over the course of 24 hours (one day) the variation is no greater than about a factor of two for any of the contaminants at the Indianapolis house or for TCE at the ASU house (when the preferential pathway was closed). The mean variability at the latter was only a bit higher (about a factor of 3) when the preferential pathway was open. In other words, a sampling protocol that involves sampling on two consecutive days would typically not uncover the large temporal variations that characterize the site over longer periods of time. As Figure 1 shows, there are certainly isolated days in which a larger daily change was observed, but these were not typical, to the extent that they fall outside of the 95% criteria used in defining the error bars. So while such unusual jumps might be seen (for unknown reasons) in a very small percentage of cases, the expectation is much more represented by what is shown in Figure 3.

Weeks of temporal separation in sampling events are required to observe the large variations of concern. Orders of magnitude differences begin to manifest themselves over the course of months. This is not surprising, since those who performed the measurements have already reported that there were seasonal aspects to the values obtained. This would be consistent with

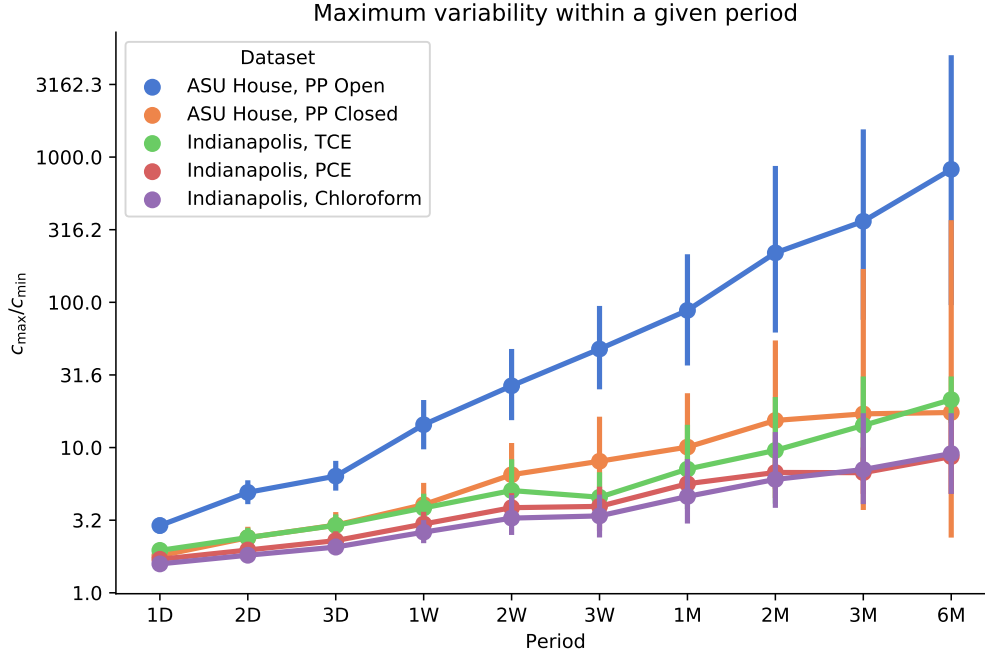


Figure 3: Mean values of the maximum change in indoor air contaminant concentration that may be expected over a given time period. (e.g., 1D is 1 day, 2W is 2 weeks, and 3M is 3 months). The error bars are the 95% confidence intervals.

218 requiring months to see the more significant variations.

219 This analysis also suggests that certain types of preferential pathways
 220 contribute to larger variations on shorter timescales (ASU House). Even
 221 though there was a preferential pathway present at the Indianapolis House,
 222 the transients associated with its presence were of a slower nature and the
 223 behavior was not unlike what was observed at ASU House when the preferen-
 224 tial pathway was closed. This warns that the mere existence of a preferen-
 225 tial pathway is not by itself sufficient to create a situation of large variations over
 226 short sampling times.

227 The longer the resampling period, the larger the maximum variability
 228 in observed indoor air contaminant concentrations. In the case of the ASU
 229 House with the preferential pathway open, the variability went from less than
 230 a threefold difference on the timescale of a day, to two to three orders of
 231 magnitude over the course of weeks. Thus there are different timescales that
 232 characterize different extents of variation, again pointing to the existence of

233 more than a single factor that determines variability.

234 Multiple samples taken over a short time period, e.g. a few days, are
235 unlikely to uncover significant variation in indoor air contaminant concen-
236 tration; the larger transient variations typically manifest after longer time
237 periods.

238 3.2. Statistical Analysis of Field Data

239 The data in Figure 1 and Figure 3 raise the question of what then actually
240 determines the large degree of temporal variation sometimes reported. The
241 rate of advective entry of soil gas into a structure is frequently cited as playing
242 an important role in determining entry rate of contaminant. This advective
243 entry rate is closely linked to the indoor-outdoor pressure difference, as can
244 be caused by the “stack effect”, for example. Thus we first consider how much
245 variability there might be in the pressure driving force for advection, and if
246 this can explain the observed variability in observed indoor air contaminant
247 concentrations.

248 The pressure difference between the indoor and outdoor/ambient ($p_{\text{in/out}}$)
249 leads to advection, by which contaminants are drawn into (or prevented from)
250 entering a structure. Changes in $p_{\text{in/out}}$ can take place quickly, leaving open
251 the possibility of their impacting VI far more rapidly than can fluctuations in
252 say groundwater depth or contaminant concentration (these latter processes
253 take weeks or even months to impact the overlying structure).

254 We examine the relationship between $p_{\text{in/out}}$ and c_{in} by constructing the
255 two-dimensional kernel density estimation (KDE) plots seen in Figure 4. The
256 KDE plots allow us to view the measured distributions of $p_{\text{in/out}}$ and c_{in} , and
257 develop a visual impression of how well these distributions correlate with one
258 another. For this analysis we considered two VI sites, NAS North Island and
259 the ASU House. The ASU House dataset was divided into two periods, one
260 before and the other after the land drain (called the preferential pathway
261 (PP) from here on) had been closed. By comparing these two periods on a
262 single plot, the impact of the preferential pathway becomes clearer.

263 In Figure 4, the indoor air contaminant concentration c_{in} is normalized to
264 the mean $c_{\text{in,mean}}$ of each dataset, allowing comparison of the impact $p_{\text{in/out}}$
265 on c_{in} independently from the large differences in absolute values of indoor
266 air concentrations at the different sites. A value of 10 on the y-axis indicates
267 that the corresponding plotted value of c_{in} is 10 times greater than the mean
268 for the dataset, and 0.1 indicate that it is one tenth of the mean.

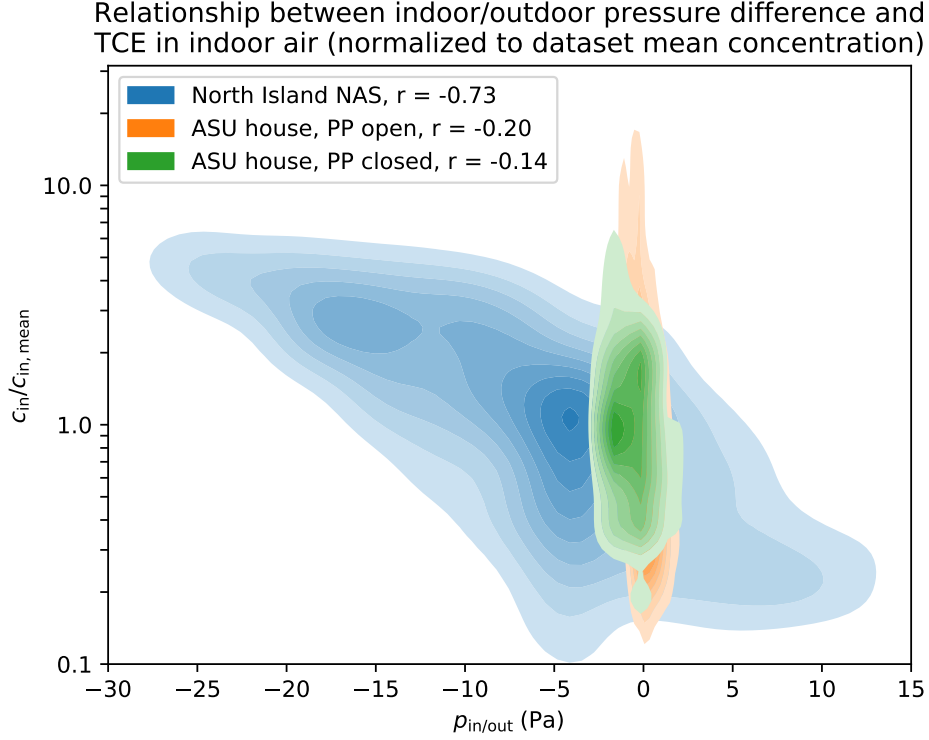


Figure 4: 2D-KDE plot showing the distributions of indoor air contaminant concentration, the indoor/outdoor pressure difference, and how they correlate to each other.

| | North Island NAS | | ASU House PP Open | | ASU House PP Closed | |
|----------------------|---------------------|------|----------------------|------|------------------------|------|
| Percentile | 5th | 95th | 5th | 95th | 5th | 95th |
| $p_{in/out}$ (Pa) | -19.9 | 7.4 | -1.4 | 2.1 | -2.1 | 2.27 |
| $c_{in}/c_{in,mean}$ | 4.1 | 0.2 | 13.5 | 0.2 | 3.3 | 0.4 |

Table 2: 5th and 95th percentile values of $p_{in/out}$ and $c_{in}/c_{in,mean}$ in Figure 4.

269 Inspection of the range of normalized c_{in} values in Figure 4 again shows
 270 the two order of magnitude spread in observed values, implying a sampling
 271 at one particular time might give a value that is two orders of magnitude
 272 different than a result from a different time. Such issues have of course
 273 already been pointed out by the investigators who obtained the data.

274 The power of this KDE representation is that it permits evaluation of the
 275 relationship of two independently measured data - the indoor air contaminant
 276 concentration and the indoor-outdoor pressure difference. Examining the
 277 data in this manner immediately points to an important difference between
 278 the data from the ASU House and those from NAS North Island. At NAS
 279 North Island site $p_{\text{in/out}}$ varies significantly; the 5th and 95th percentile of
 280 $p_{\text{in/out}}$ are -19.9 and 7.4 Pa respectively. This may be contrasted with 5th
 281 and 95th percentile $p_{\text{in/out}}$ at the ASU house: -1.4 and 2.1 Pa (with the PP
 282 open), and -2.1 and 2.27 Pa (PP closed).

283 The much larger under- and overpressurization of the NAS North Island
 284 site compared to the ASU House makes the pressure dependence of indoor
 285 air concentration much more visible at the former site. The Pearson's r-value
 286 for the correlation between $p_{\text{in/out}}$ and c_{in} for each dataset is shown in the
 287 legend, and confirms what is apparent to the eye; the pressure driving force is
 288 a determining factor for observed contamination at NAS North Island. But
 289 the broadness of the band of the NAS North Island concentration data set
 290 suggests that there is still a source of variability in c_{in} that has not been fully
 291 captured - this will be addressed below.

292 The ASU house datasets offer a different picture. The variability of c_{in} is
 293 just as large, or even larger than at NAS North Island, yet the $p_{\text{in/out}}$ varied
 294 far less. The weaker dependence of c_{in} on the pressure difference is confirmed
 295 by the much lower r-values for the correlations between the variables. In
 296 other words, there is not nearly as strong a correlation between variation in
 297 indoor air contaminant concentration and pressure difference for the ASU
 298 House as there was for NAS North Island. These results strongly suggest
 299 that there are other factors besides indoor pressure determining indoor air
 300 contaminant concentrations, and their variations, that may not be accounted
 301 for in applying this method.

302 The data for the ASU House also offer an insight into the role of the
 303 preferential pathway. At first glance it may seem like the c_{in} values for the
 304 periods when the PP is open and closed are relatively comparable. However,
 305 the 5th and 95th percentiles values of $c_{\text{in}}/c_{\text{in,mean}}$ differ significantly as may
 306 be seen in Table 2. It is clear that existence of the preferential pathway
 307 dramatically increases the variability in indoor air contaminant concentra-
 308 tion. This again is entirely consistent with what the investigators of that
 309 site have already reported[11]. The correlation with indoor-outdoor pressure
 310 difference is weak in the ASU house cases, so there are clearly factors other
 311 than pressure difference that determine the variability in each. These will be

312 explored with the help of a modeling analysis presented below.

313 3.3. Variability Of Attenuation to Subslab Concentrations

314 Observed temporal variations in indoor air contaminant concentrations
315 might be explained by temporal variations in subslab contaminant concen-
316 trations. To examine how variability in subslab contaminant concentration
317 might contribute to variability in indoor air contaminant concentration, data
318 on the attenuation from subslab ($\alpha_{\text{subslab}} = c_{\text{in}}/c_{\text{subslab}}$) were examined. The
319 dataset utilized for this was that from the ASU House. The c_{subslab} values
320 were taken from a soil gas probe labeled as "6" at the ASU house. This probe
321 was located closest to both the exit of the preferential pathway pipe, and to
322 a reported breach in the foundation that served as a key entry pathway for
323 contaminant getting into the house[11]. The results are shown in Figure 5,
324 which shows the full distributions for both the case in which the preferential
325 pathway was "open" and when it "closed".

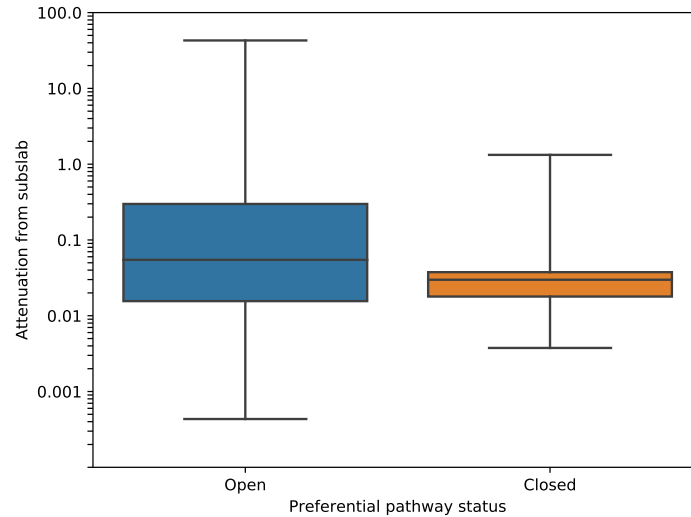


Figure 5: Boxplot of \log_{10} (subslab to indoor air contaminant attenuation) at the ASU house site. The box shows the quartiles of the distribution, the whiskers the extent of the distribution.

326 It is apparent that during the period when the preferential pathway was
327 closed, α_{subslab} did not vary significantly, and was quite close to the EPA
328 recommended α_{subslab} value of 0.03[1]. Thus during the period when the

329 preferential pathway was closed, large temporal variations in subslab concen-
330 trations could not have been driving the variations in indoor air contaminant
331 concentrations.

332 When the PP was open, there was considerably more variability in the
333 subslab concentration values, and the mean value was higher than in the
334 case where the preferential pathway was closed. It was also not uncommon
335 for the observed α_{subslab} to exceed unity. While large α_{subslab} values may
336 sometimes indicate indoor sources at a site, there were none at the ASU
337 house. A more likely explanation is that even though probe "6" was located
338 in close proximity to the exit of the preferential pathway, there might have
339 still existed significant spatial variability in c_{subslab} that could not be captured
340 with a single measurement. This suggests caution is needed in profiling
341 subslab contaminant concentrations in the presence of preferential pathways
342 - significant variations are possible.

343 What the results of Figure 5 do clearly show is that the existence of a
344 preferential pathway of the kind at ASU House (and idealized in Figure 1)
345 can influence the temporal variation of subslab concentrations in a much less
346 predictable way than those observed in "normal" VI scenarios.

347 3.4. Modeling Results

348 3.4.1. Pressure Effects

349 Having established the potential impacts of certain inputs on determining
350 variability in indoor air contaminant concentrations, the mathematical model
351 of VI can help further elucidate other key aspects. The results of calculations
352 on a scenario corresponding to Figure 2 are presented in Figure 6. This
353 scenario is not intended to exactly represent the situation at ASU House,
354 but it is similar in the key aspect of having a preferential pathway delivering
355 contaminant to a gravel sub-base. The full, complex geometry of the ASU
356 House has not been represented, but the modeled structure is of comparable
357 size, and will be subject to operational parameters based upon what were
358 measured at that site. The general modeling conditions are those shown in
359 Table 1.

360 In the calculation results shown in the top panel of Figure 6, a prefer-
361 ential pathway is assumed to provide air containing contaminant vapor at
362 a concentration equivalent to the vapor in equilibrium with the underlying
363 groundwater source. Here, the indoor air exchange rate A_e was assumed to
364 be a constant 0.5 per hour, and $p_{\text{in/out}}$ was varied from -5 to 5 Pa. Values
365 of predicted indoor air contaminant concentrations, c_{in} were obtained from

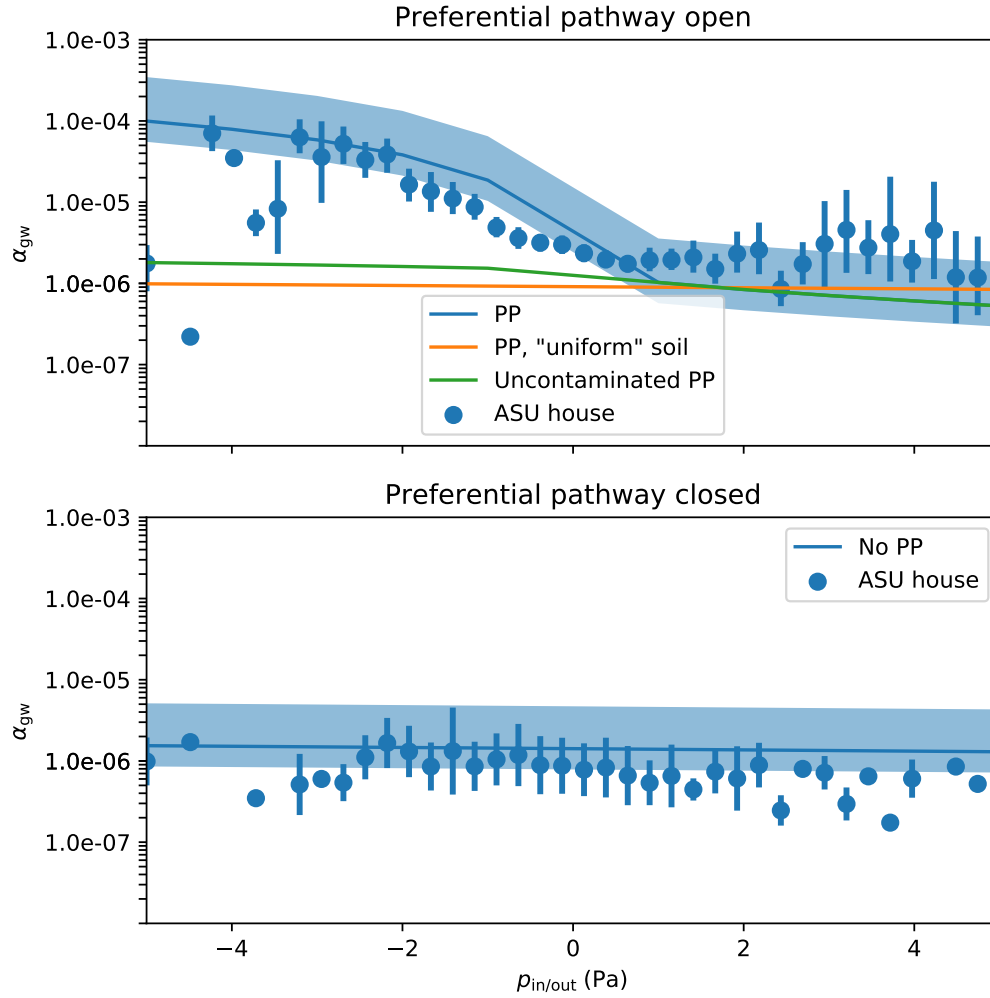


Figure 6: Simulated preferential pathway scenarios compared to actual ASU house field data. Field data are binned in 40 evenly spaced pressure bins, with the dot representing the mean and errors bars the 95% confidence interval of data at a particular pressure range. Shaded blue represent the range of model predictions for the indicated pressure difference, due to air exchange rate variability (using 5th and 95th percentile values of measured exchange rates). Top panel is for various cases representing an "open" preferential pathway, the lower panel with the pathway "closed".

366 steady state calculations. The predicted c_{in} values were then normalized by
 367 the assumed vapor concentration in equilibrium with groundwater c_{gw} , giving
 368 the attenuation from groundwater α_{gw} . The predicted values of α_{gw} as a

function of $p_{\text{in/out}}$ are given by the central blue line in the upper panel of Figure 6. These predicted values are compared to actual measured α_{gw} values from the ASU House for the period during which the preferential pathway was open (blue points).

The model successfully predicts the observed trends in α_{gw} as $p_{\text{in/out}}$ decreases (increased depressurization) but somewhat underpredicts α_{gw} as the house is overpressurized. Most significantly, the model captures that even for a small increase in depressurization (0 to -5 Pa) a very large increase in α_{gw} (two order of magnitude) can occur.

The asymmetry relative to the predictions for depressurization and overpressurization is due to two factors. First, the preferential pathway acts not only as a source of contaminant vapor, but also as a source of air to the subslab. Because of the large resistance to soil gas flow in the surrounding soil, having a local source of air to support the increase of advective flow into the structure from the subslab region makes a large difference.

The above was proven by a second simulation, where the model was rerun with the preferential pathway present, but with the permeable (gravel) layer in the subslab removed and replaced by the surrounding soil (sandy loam). This gave a "uniform soil" scenario the results of which are shown as an orange line in the top panel of Figure 6. This simulation demonstrates that without a permeable subslab to effectively allow the "advective potential" to be realized, existence of preferential pathway will actually not impact a VI site very much. In order for a preferential pathway to significantly contribute to VI, this requires a scenario involving good advective communication between it the indoor environment. These requirements were met at the ASU House.

A perhaps obvious second requirement is that the preferential pathway must deliver contaminant vapors to be impactful. In another simulation, the permeable (gravel) subslab region was included, but the preferential pathway merely delivered clean air to the subslab. The result of this simulation is shown as the green line in the top panel of Figure 6. This shows that while there was a lightly larger α_{gw} compared to the "uniform soil" scenario, it is nowhere near as significant as when the preferential pathway delivers contaminant vapors. The contaminated and uncontaminated preferential pathway scenarios (blue and green lines respectively) thus bound the range of α_{gw} that would be observed for a given $p_{\text{in/out}}$ depending on the contaminant vapor concentration in the preferential pathway.

The model is also able to capture the weak trend in α_{gw} with $p_{\text{in/out}}$ when

407 a preferential pathway is absent, but when there still exists a permeable
 408 subslab region. These results are shown in the bottom panel of Figure 6.
 409 These results are again in agreement with what was observed at the ASU
 410 House when the preferential pathway was closed, i.e. that there was a much
 411 more modest variation in indoor air concentration, irrespective of pressure,
 412 when the preferential pathway was cut off.

413 The above simulations capture the trend in α_{gw} with $p_{\text{in/out}}$ but do not yet
 414 capture the full variability of the concentration results over the "most prob-
 415 able" portion of observed pressure distributions shown in Figure 4 (which
 416 tend to be from -2 to +2 Pa). The results of Figure 6 show a spread of
 417 almost an order of magnitude over this pressure range for the case of the
 418 "open" preferential pathway, and almost no spread at all when the prefer-
 419 ential pathway is "closed". Hence the predicted variability is roughly an
 420 order of magnitude too low, when considering only the influence of pressure.
 421 There is a factor that tends to increase the spread of the data one additional
 422 order of magnitude beyond what was predicted by the base calculations of
 423 Figure 6. We believe that it is variations in air exchange rate, operating in
 424 concert with the natural variations in pressure differential, that explain the
 425 remaining variability.

426 3.4.2. Air Exchange Rate Effects

427 Table 3 shows the observed variations in air exchange rates for the ASU
 428 House and Indianapolis House, compared with EPA's summary of the dis-
 429 tribution of typical residential air exchange rates[29, 30]. Examination of
 430 these distributions point in a clear direction for modifying the above model.
 431 Instead of using a constant value of air exchange rate, as is customary, its
 432 values should be parameterized. A higher air exchange would of course be
 433 associated with lower c_{in} and vice versa. Moreover, A_e may sometimes be
 434 correlated with $p_{\text{in/out}}$. Determining any general relationship between A_e and
 435 $p_{\text{in/out}}$ is difficult: the structure itself and weather phenomena have a signifi-
 436 cant effect on air exchange. As the data in Figure 7 show, there is no easily
 437 discernable correlation between these variables at the ASU site, though there
 438 is a hint of slight seasonal dependence. Note: a relationship between A_e and
 439 $p_{\text{in/out}}$ may be established for larger $p_{\text{in/out}}$ via the building leakage curves,
 440 which are widely used for heating, ventilation and air conditioning systems
 441 in construction.

442 To show the influence of possible statistical fluctuations of air exchange
 443 rate on the predictions of α_{gw} values, the scenarios of Figure 6 were rerun

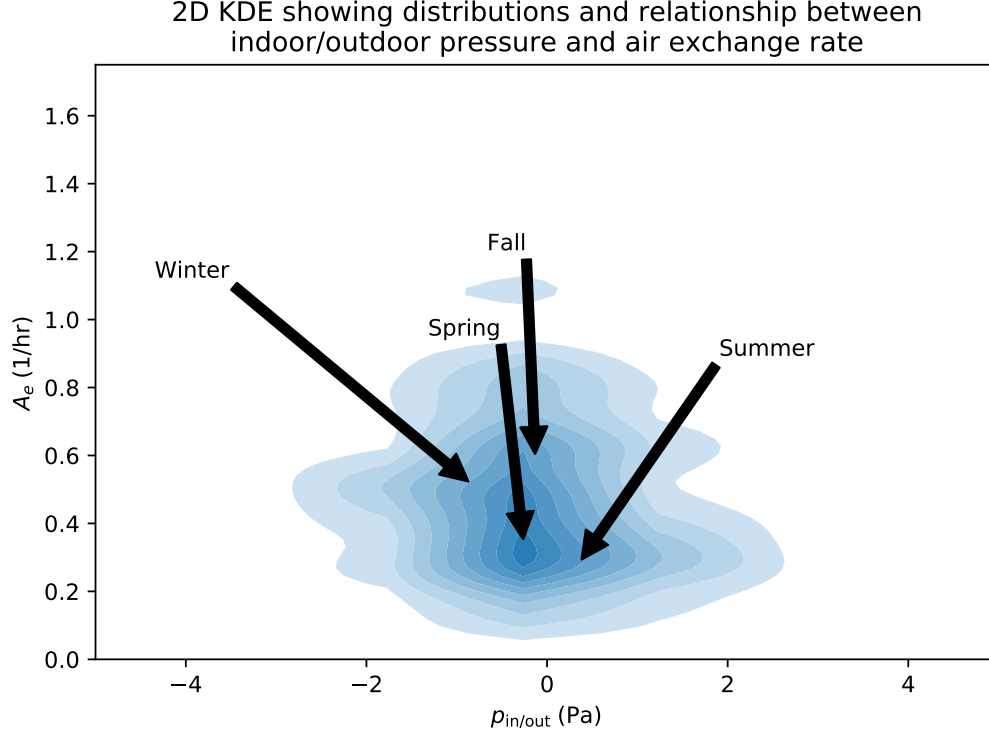


Figure 7: 2D KDE figure showing distributions and relationship between indoor/outdoor pressure difference and air exchange rate. The seasonal median $p_{in/out}$ and A_e are indicated by the location of the respective arrow tips. Only non-CPM period considered.

| Percentile | 10th | 50th | 90th |
|------------------|----------|-----------|-----------|
| EPA[29, 30] | 0.16-0.2 | 0.35-0.49 | 1.21-1.49 |
| ASU house[3, 11] | 0.21 | 0.43 | 0.78 |
| Indianapolis[7] | 0.34 | 0.74 | 1.27 |

Table 3: Air exchange rate values (1/hr)

calculated using the 5th and 95th percentile measured A_e values, 0.17 and 0.90 respectively (based upon the actual distributions in Figure S1), providing predicted upper and lower bounds for α_{gw} . These bounds are indicated by the shaded blue regions around the center line calculated for an assumed constant A_e of 0.5 per hour.

It is apparent that assuming variability in air exchange rate allows cap-

450 turing most of the observed variability in α_{gw} . We believe that this explains
 451 the portion of the variation in indoor air contaminant concentration data
 452 that cannot be explained by either existence of preferential pathways or by
 453 the range in indoor depressurization. Thus, we believe that it is the inter-
 454 play of preferential pathway conditions, with indoor pressure variations and
 455 normal air exchange rates that help to explain the observations of significant
 456 variations in reported indoor air contaminant concentrations.

457 3.4.3. Results of Transient Simulations

458 The above analyses have been conducted under simulated steady state
 459 conditions. The conclusions regarding the importance of the different pa-
 460 rameters are now examined in actual transient simulations. The model con-
 461 figuration of Figure 2 is run in 24-hour transient simulations to examine how
 462 c_{in} fluctuates over the course of a "typical" day. The simulations vary $p_{\text{in/out}}$
 463 as one model input, and then assume either a constant or time-varying air
 464 exchange rate, A_e . The ASU House dataset was again the source of the "typ-
 465 ical" $p_{\text{in/out}}$ temporal variation, obtained by examining the median, hourly,
 466 diurnal $p_{\text{in/out}}$ during the non-CPM periods. The statistically "typical" $p_{\text{in/out}}$
 467 cycle may be seen in the upper left panel of Figure 8 (note that values be-
 468 tween the hourly median values are interpolated using cubic splines). The
 469 "typical" air exchange rate is calculated in exactly the same way and is shown
 470 by the blue line in the upper right panel of Figure 8. The orange line is the
 471 air exchange rate value assumed for the calculations at constant air exchange
 472 rate.

473 The result of these simulations are shown in the bottom two panels of
 474 Figure 8, where the left and right panels show the results of open and closed
 475 preferential pathways, respectively. The "max change" value in the legends
 476 is the quotient of the lowest and highest predicted concentrations, i.e. a value
 477 of two indicate that the maximum daily concentration is twice as high as the
 478 lowest. This quantity may be compared with the value that is plotted for
 479 "one day" in Figure 3. When the preferential pathway is open, there is a
 480 maximum daily variation of roughly a factor of 5, irrespective of whether A_e
 481 fluctuates or not, which is somewhat more than the maximum daily varia-
 482 tion shown in Figure 3. The relatively small difference between the variable
 483 and constant A_e cases indicates that most of the variability during a "typi-
 484 cal" day is here attributable to fluctuations in $p_{\text{in/out}}$, i.e. the contaminant
 485 transport into the modeled structure is advection dominated. Even for the
 486 small fluctuations in $p_{\text{in/out}}$ the contaminant entry rate fluctuation drives

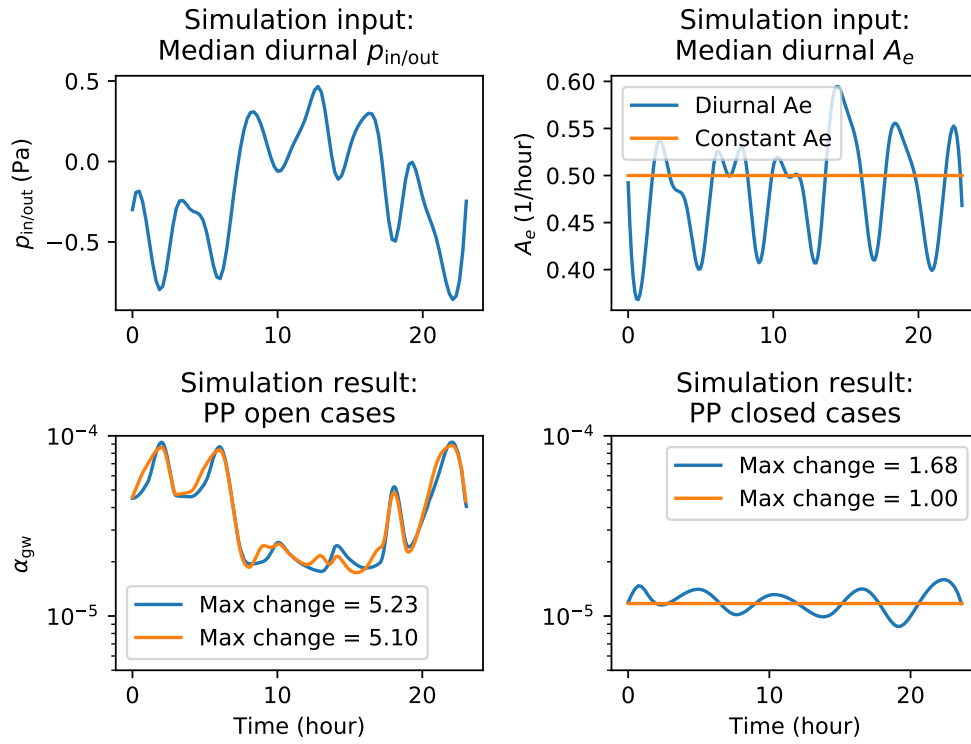


Figure 8: Transient simulation of a "typical" VI day, using diurnal indoor/outdoor pressure difference and air exchange rate as inputs. Effect of preferential pathway considered.

the observed indoor concentration. When the preferential pathway is closed the story is quite different. When air exchange rate is held constant, there is essentially no variation in c_{in} . This is again not surprising, as Figure 6 demonstrated that when the preferential pathway is closed, the influence of $p_{in/out}$ on contaminant entry rate (and subsequently c_{in}) is small. Combined with the small $p_{in/out}$ this indicates that the contaminant transport into the modeled structure in this scenario is dominated by diffusion. When the air exchange rate is allowed to fluctuate, the maximum daily variation in c_{in} is 1.68, which is in line with what is shown in Figure 3. This shows that for a "typical" day, when the preferential pathway is closed off, much of the daily variation in c_{in} is due to daily fluctuations in air exchange rate.

These results demonstrate the complicated nature of temporal variability in c_{in} . It is important to recall that only the effects of indoor/outdoor pressure difference and air exchange rate have been considered here, but slower processes, e.g. changes in groundwater contaminant concentration or various seasonal effects can also have a significant impact on VI over time. For the shorter time periods of concern in recent studies of temporal variability in indoor contaminant concentrations we believe that these are dominated by combinations of indoor/outdoor pressure differentials and air exchange rate. For a site where advective communication between the subsurface and the indoor is good, $p_{in/out}$ is likely a significant determinant of c_{in} and its temporal variability. We have shown that that such a scenario may arise due to a preferential pathway entering a permeable sub-base, but may also exist even in the absence of a preferential pathway just as the results from NAS North Island demonstrate. At sites where advective transport into the structure is limited, much of the temporal variability in c_{in} may be attributed to natural fluctuations in air exchange rate.

4. Conclusions

Based on statistical analysis of field data from vapor intrusion sites showing significant temporal variations in indoor air contaminant concentrations, supplemented by computational fluid dynamics modeling, it is concluded that several different factors can play a role in determining these variations.

There can be a significant role of advective transport in determining observed variability. For advective transport to play a decisive role, the present results show that there must exist a sub-foundation zone that permits significant flow of soil gas. In the case of NAS North Island, a relatively permeable

523 sub-foundation soil permitted fairly high variations in building indoor pres-
524 sure to cause significant fluctuations in contaminant entry rate. In the case
525 of the ASU house, a permeable gravel sub-base allowed good communication
526 of the indoor air environment with the contents of a preferential contaminant
527 pathway that entered that sub-base, even though the pressure driving force
528 was not nearly as large as that at NAS North Island. Both situations led
529 to well-documented large variations (two or three orders of magnitude) in
530 indoor air contaminant concentrations.

531 Modeling work has shown that the existence of preferential pathways that
532 communicate with a permeable sub-slab zone can create significant spatial
533 variability in contaminant concentration in the subslab. In other words, the
534 existence of a permeable sub-slab layer (such as gravel) does not assure that
535 there will exist a well-mixed sub-slab zone. This warns that taking isolated
536 subslab vapor samples may be misleading, as a result of spatial variability of
537 contaminant concentrations. This might in turn lead to apparent attenuation
538 from the sub-slab to indoors that appears to exceed the EPA recommended
539 value of 0.03 and even exceed unity - potentially leading to the erroneous
540 conclusion that an indoor source is present.

541 In the absence of a preferential pathway (a situation that existed at the
542 ASU house when the pathway was closed off) and in the presence of only
543 a modest observed pressure driving force, there was still observed a signifi-
544 cant temporal variation in indoor air contaminant concentration of around
545 an order of magnitude. Statistical analysis of that data set showed, how-
546 ever, that indoor air contaminant concentrations were actually unlikely to
547 vary by more than a factor of three over a week-long or shorter sampling
548 period. The small variability that was seen over these short times could be
549 explained by inherent variability in air exchange rates. It was when indoor
550 air samples taken over longer periods were compared that an almost order
551 of magnitude variation became apparent. These results were consistent with
552 seasonal timescale variations in the intrusion processes.

553 **Acknowledgements**

554 This project was supported by grant ES-201502 from the Strategic Envi-
555 ronmental Research and Development Program and Environmental Security
556 Technology Certification Program (SERDP-ESTCP).

557 Declaration of interest: none

| | |
|-----------------------|---|
| A_{ck} | Crack area |
| A_e | Air exchange rate |
| α, n, m, l | van Genuchten parameters |
| α_{gw} | Attenuation from groundwater contaminant vapor source |
| c_{in} | Indoor air contaminant concentration |
| c | Soil-gas contaminant concentration |
| c_w | Soil-water contaminant concentration |
| c_{gw} | Contaminant groundwater concentration |
| χ | PP contaminant concentration scaling parameter |
| D_{eff} | Effective diffusion coefficient |
| D_{air} | Diffusion coefficient in air |
| D_{water} | Diffusion coefficient in water |
| \dot{j}_{ck} | Contaminant molar flux through the foundation crack |
| κ_s | Saturated soil permeability |
| K_H | Dimensionless Henry's law constant |
| k_r | Relative permeability |
| L_{slab} | Thickness of the foundation slab |
| M | Molar mass |
| μ | Contaminant vapor viscosity |
| NAS | Naval Air Stations |
| p | Pressure in soil |
| $p_{\text{in/out}}$ | Indoor/outdoor pressure difference |
| PP | Preferential pathway |
| ρ | Density |
| Se | Soil water saturation |
| t | time |
| θ_g | Vapor/gas filled porosity |
| θ_w | Water filled porosity |
| θ_r | Residual water filled porosity |
| θ_t | Total porosity |
| \vec{u} | Soil-gas velocity (vector quantity) |
| VI | Vapor intrusion |
| V_{base} | Basement volume |
| z | Elevation above groundwater |

Table 4: List of abbreviations and nomenclature

References

- [1] U.S. Environmental Protection Agency, OSWER Technical Guide for Assessing and Mitigating the Vapor Intrusion Pathway From Subsurface Vapor Sources To Indoor Air (2015).
- [2] D. Folkes, W. Wertz, J. Kurtz, T. Kuehster, Observed Spatial and Temporal Distributions of CVOCs at Colorado and New York Vapor Intrusion Sites, *Ground Water Monitoring & Remediation* 29 (1) (2009) 70–80. doi:10/fw6kxz.
- [3] C. Holton, H. Luo, P. Dahlen, K. Gorder, E. Dettenmaier, P. C. Johnson, Temporal Variability of Indoor Air Concentrations under Natural Conditions in a House Overlying a Dilute Chlorinated Solvent Groundwater Plume, *Environmental Science & Technology* 47 (23) (2013) 13347–13354. doi:10/gd6dfd.
- [4] J. E. Johnston, J. M. Gibson, Spatiotemporal variability of tetrachloroethylene in residential indoor air due to vapor intrusion: A longitudinal, community-based study, *Journal of Exposure Science and Environmental Epidemiology* 24 (6) (2014) 564. doi:10/f6m5wc.
- [5] V. Hosangadi, B. Shaver, B. Hartman, M. Pound, M. L. Kram, C. Frescura, High-Frequency Continuous Monitoring to Track Vapor Intrusion Resulting From Naturally Occurring Pressure Dynamics, *Remediation Journal* 27 (2) (2017) 9–25. doi:10/gd6df5.
- [6] T. McHugh, P. Loll, B. Eklund, Recent advances in vapor intrusion site investigations, *Journal of Environmental Management* 204 (2017) 783–792. doi:10/gd6dgk.
- [7] U.S. Environmental Protection Agency, Assessment of Mitigation Systems on Vapor Intrusion: Temporal Trends, Attenuation Factors, and Contaminant Migration Routes under Mitigated And Non-mitigated Conditions (2015).
- [8] P. C. Johnson, C. W. Holton, Y. Guo, P. Dahlen, E. H. Luo, K. Gorder, E. Dettenmaier, R. E. Hinchey, Integrated Field-Scale, Lab-Scale, and Modeling Studies for Improving Our Ability to Assess the Groundwater to Indoor Air Pathway at Chlorinated Solvent-Impacted Groundwater Sites (2016).

- 591 [9] C. W. Holton, Evaluation of Vapor Intrusion Pathway Assessment
592 Through Long-Term Monitoring Studies, PhD Thesis, Arizona State
593 University (2015).
- 594 [10] Y. Guo, Vapor Intrusion at a Site with an Alternative Pathway and a
595 Fluctuating Groundwater Table, PhD Thesis, Arizona State University
596 (2015).
- 597 [11] Y. Guo, C. Holton, H. Luo, P. Dahlen, K. Gorder, E. Dettenmaier,
598 P. C. Johnson, Identification of Alternative Vapor Intrusion Pathways
599 Using Controlled Pressure Testing, Soil Gas Monitoring, and Screening
600 Model Calculations, *Environmental Science & Technology* 49 (22) (2015)
601 13472–13482. doi:10/f72b6n.
- 602 [12] T. McHugh, L. Beckley, T. Sullivan, C. Lutes, R. Truesdale, R. Uppen-
603 camp, B. Cosky, J. Zimmerman, B. Schumacher, Evidence of a sewer
604 vapor transport pathway at the USEPA vapor intrusion research duplex,
605 *Science of The Total Environment* 598 (2017) 772–779. doi:10/gd6dfz.
- 606 [13] K. G. Pennell, M. K. Scammell, M. D. McClean, J. Ames, B. Weldon,
607 L. Friguglietti, E. M. Suuberg, R. Shen, P. A. Indeglia, W. J. Heiger-
608 Bernays, Sewer Gas: An Indoor Air Source of PCE to Consider During
609 Vapor Intrusion Investigations, *Groundwater Monitoring & Remedia-
610 tion* 33 (3) (2013) 119–126. doi:10/gd6dd9.
- 611 [14] M. Roghani, O. P. Jacobs, A. Miller, E. J. Willett, J. A. Jacobs, C. R.
612 Viteri, E. Shirazi, K. G. Pennell, Occurrence of chlorinated volatile or-
613 ganic compounds (VOCs) in a sanitary sewer system: Implications for
614 assessing vapor intrusion alternative pathways, *Science of The Total En-
615 vironment* 616-617 (2018) 1149–1162. doi:10/gd6dgh.
- 616 [15] C. E. Riis, A. G. Christensen, M. H. Hansen, H. Husum, M. Terkelsen,
617 Vapor intrusion through sewer systems: Migration pathways of chlori-
618 nated solvents from groundwater to indoor air (May 2010).
- 619 [16] K. B. Nielsen, B. Hvidberg, Remediation techniques for mitigating vapor
620 intrusion from sewer systems to indoor air, *Remediation Journal* 27 (3)
621 (2017) 67–73. doi:10/gd6ddz.
- 622 [17] D. Brenner, Results of a Long-Term Study of Vapor Intrusion at
623 Four Large Buildings at the NASA Ames Research Center, *Journal*

- 624 of the Air & Waste Management Association 60 (6) (2010) 747–758.
625 doi:10/bs8wxx.
- 626 [18] T. E. McHugh, L. Beckley, D. Bailey, K. Gorder, E. Dettenmaier,
627 I. Rivera-Duarte, S. Brock, I. C. MacGregor, Evaluation of Vapor In-
628 trusion Using Controlled Building Pressure, *Environmental Science &*
629 *Technology* 46 (9) (2012) 4792–4799. doi:10/f3xdtm.
- 630 [19] E. Jones, T. Oliphant, Pearu Peterson, *SciPy: Open source scientific*
631 *tools for Python* (2011).
- 632 [20] R. Shen, K. G. Pennell, E. M. Suuberg, Influence of Soil Moisture on
633 Soil Gas Vapor Concentration for Vapor Intrusion, *Environmental En-*
634 *gineering Science* 30 (10) (2013) 628–637. doi:10/gd6dfc.
- 635 [21] Y. Yao, Y. Wang, Z. Zhong, M. Tang, E. M. Suuberg, Investigating
636 the Role of Soil Texture in Vapor Intrusion from Groundwater Sources,
637 *Journal of Environmental Quality* 46 (4) (2017) 776–784. doi:10/gbrx64.
- 638 [22] Y. Yao, F. Mao, S. Ma, Y. Yao, E. M. Suuberg, X. Tang, Three-
639 Dimensional Simulation of Land Drains as a Preferential Pathway for
640 Vapor Intrusion into Buildings, *Journal of Environmental Quality* 46 (6)
641 (2017) 1424–1433. doi:10/gcnw26.
- 642 [23] L. A. Richards, Capillary conduction of liquids through porous mediums,
643 *Physics* 1 (5) (1931) 318–333. doi:10/ccmx4x.
- 644 [24] M. T. van Genuchten, A Closed-form Equation for Predicting the Hy-
645 draulic Conductivity of Unsaturated Soils, *Soil Science Society of Amer-*
646 *ican* 44 (5) (1980) 892–898. doi:10/fdc8mc.
- 647 [25] R. J. Millington, J. P. Quirk, Permeability of porous solids, *Transactions*
648 *of the Faraday Society* 57 (0) (1961) 1200. doi:10/btx653.
- 649 [26] H.-C. Dan, P. Xin, L. Li, L. Li, D. Lockington, Capillary effect on flow
650 in the drainage layer of highway pavement, *Canadian Journal of Civil*
651 *Engineering* 39 (6) (2012) 654–666. doi:10/f3236b.
- 652 [27] L. D. V. Abreu, H. Schuver, *Conceptual Model Scenarios for the Vapor*
653 *Intrusion Pathway* (2012).

- 654 [28] U.S. Environmental Protection Agency, Users's Guide For Evaluating
655 Subsurface Vapor Intrusion Into Buildings (2004).
- 656 [29] U.S. EPA, Exposure Factors Handbook 2011 Edition, Tech. rep., U.S.
657 Environmental Protection Agency (2011).
- 658 [30] M. D. Koontz, H. E. Rector, Estimation of Distributions for Residential
659 Air Exchange Rates, Tech. rep., U.S. Environmental Protection Agency
660 (Mar. 1995).